

Study of uranium nuclei deformation at STAR

Chunjian Zhang

Session H14.00004

March 18, 2021

Supported in part by

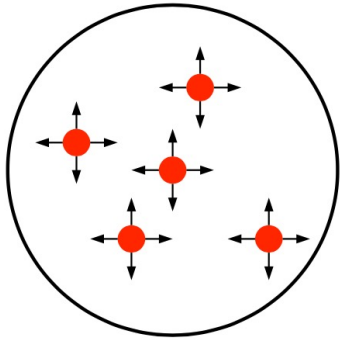


Connecting the initial state to the nuclear geometry

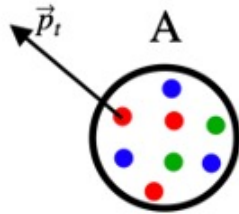
- System size affects the transverse momentum of particles

- Shape affects anisotropic flow of particles

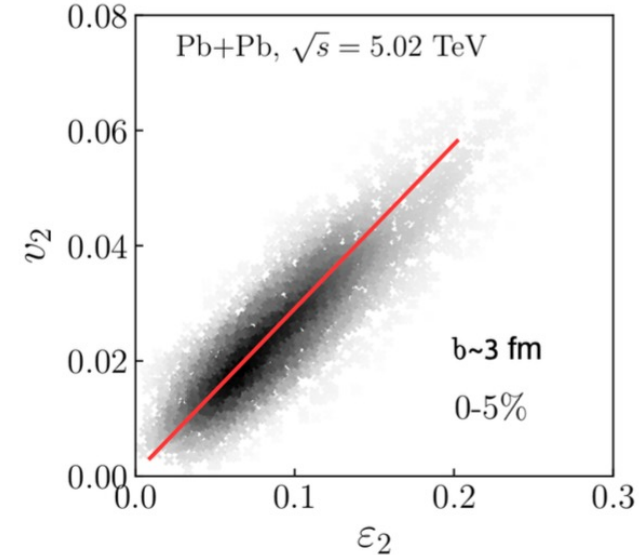
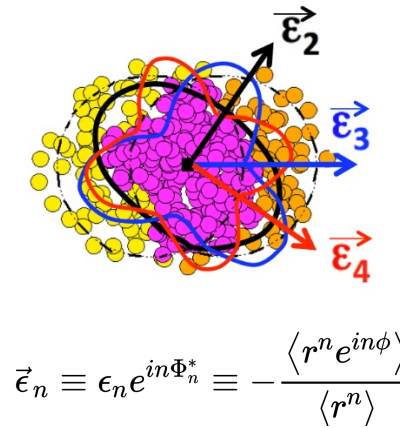
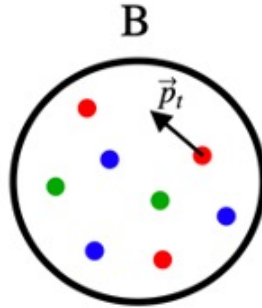
initial density profile



small R, large $\langle p_T \rangle$



large R, small $\langle p_T \rangle$



$$\vec{\epsilon}_n \equiv \epsilon_n e^{in\Phi_n^*} \equiv -\frac{\langle r^n e^{in\phi} \rangle}{\langle r^n \rangle}$$

$$v_n \propto \epsilon_n, n = 2, 3$$

$$\langle p_T \rangle \sim 1/R$$

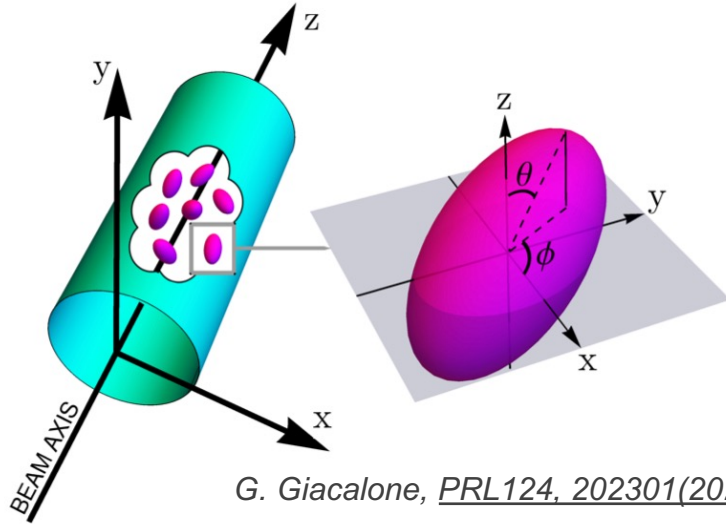
$$c_s^2 = \frac{dP}{d\epsilon} = \frac{d \ln T}{d \ln s} = \frac{d \ln \langle p_T \rangle}{d \ln N_{ch}}$$

$$\frac{d \langle p_T \rangle}{\langle \langle p_T \rangle \rangle} = -3c_s^2 \frac{dR}{\langle R \rangle}$$

(Hydrodynamic approximation)

The fluctuation in size and shape are related to mean p_T fluctuation and v_n .

Connecting the initial state to the nuclear geometry

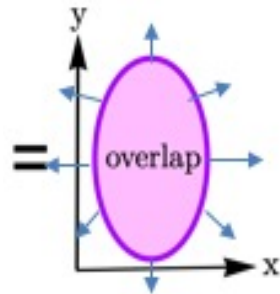
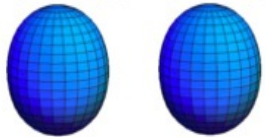


For a deformed nucleus, the leading form of nuclear density becomes:

$$\rho(r, \theta) = \frac{\rho_0}{1 + e^{(r - R_0(1 + \beta_2 Y_{20}(\theta)))/a}} \quad Y_{20} = \sqrt{\frac{5}{16\pi}} (3 \cos^2 \theta - 1)$$

Deformation is dominated by quadrupole component β_2

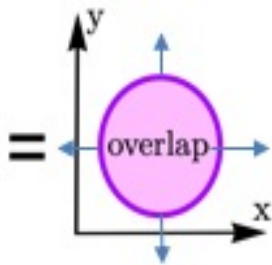
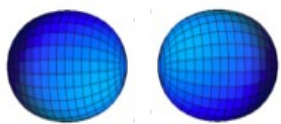
Body-Body



large R , small $\langle p_T \rangle$
large ϵ_2

Prolate nuclei

Tip-Tip



small R , large $\langle p_T \rangle$
small ϵ_2

Ultra-central collisions

- ϵ_2 and R are influenced by the quadrupole deformation β_2

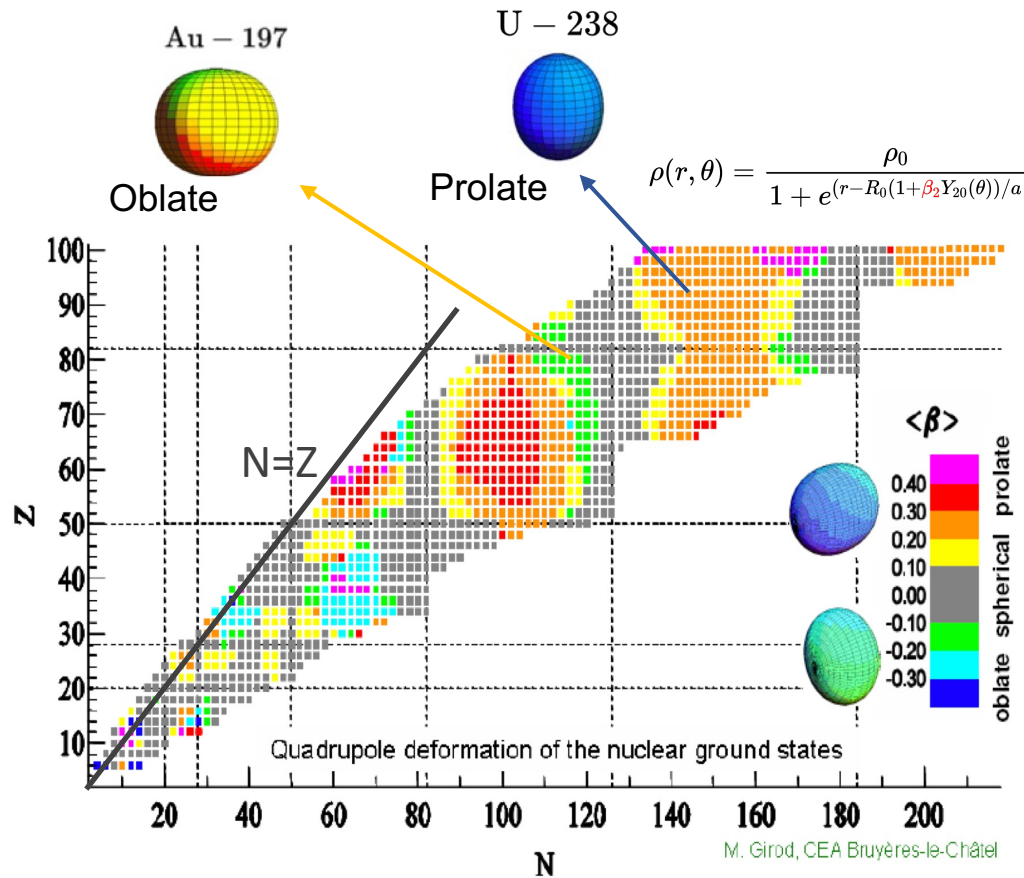
- $\langle p_T \rangle \sim 1/R$ and $v_2 \propto \epsilon_2$:

deformation contributes to anticorrelation between v_2 and $\langle p_T \rangle$

Measuring the $v_2 - \langle p_T \rangle$ correlation could reveal the quadrupole deformation β_2 . ³

Quadrupole deformations β_2 of different nuclei

A. Gorgen, *Tech. Rep. 051, 019(2015)*



Hartree-Fock-Bogolyubov (Gogny D1S effective interaction)

A few values based on the nuclear structure approximations

The β_2 of ^{238}U has a large value:

reference	Raman et al.	Löbner et al.	Möller et al.	Möller et al.	CEA DAM	Bender et al.
method	exp	exp	FRDM	FRLDM	HFB	“beyond mean field”
β_2	0.286	0.281	0.215	0.236	0.30	0.29

[Raman et al., ADNDT78,1(2001)]

[Möller et al., ADNDT59,185(1995)]

[Hilaire & Girod, EPJA(2007)]

[Löbner et al., NDT A7, 495 (1970)]

[Möller et al., 1508.06294]

[Bender et al., nucl-th/0508052]

The β_2 of ^{179}Au is small and can be used as baseline

reference	Möller et al.	Möller et al.	CEA DAM
method	FRDM	FRLDM	HFB
β_2	-0.131	-0.125	-0.10

[Möller et al., 1508.06294]

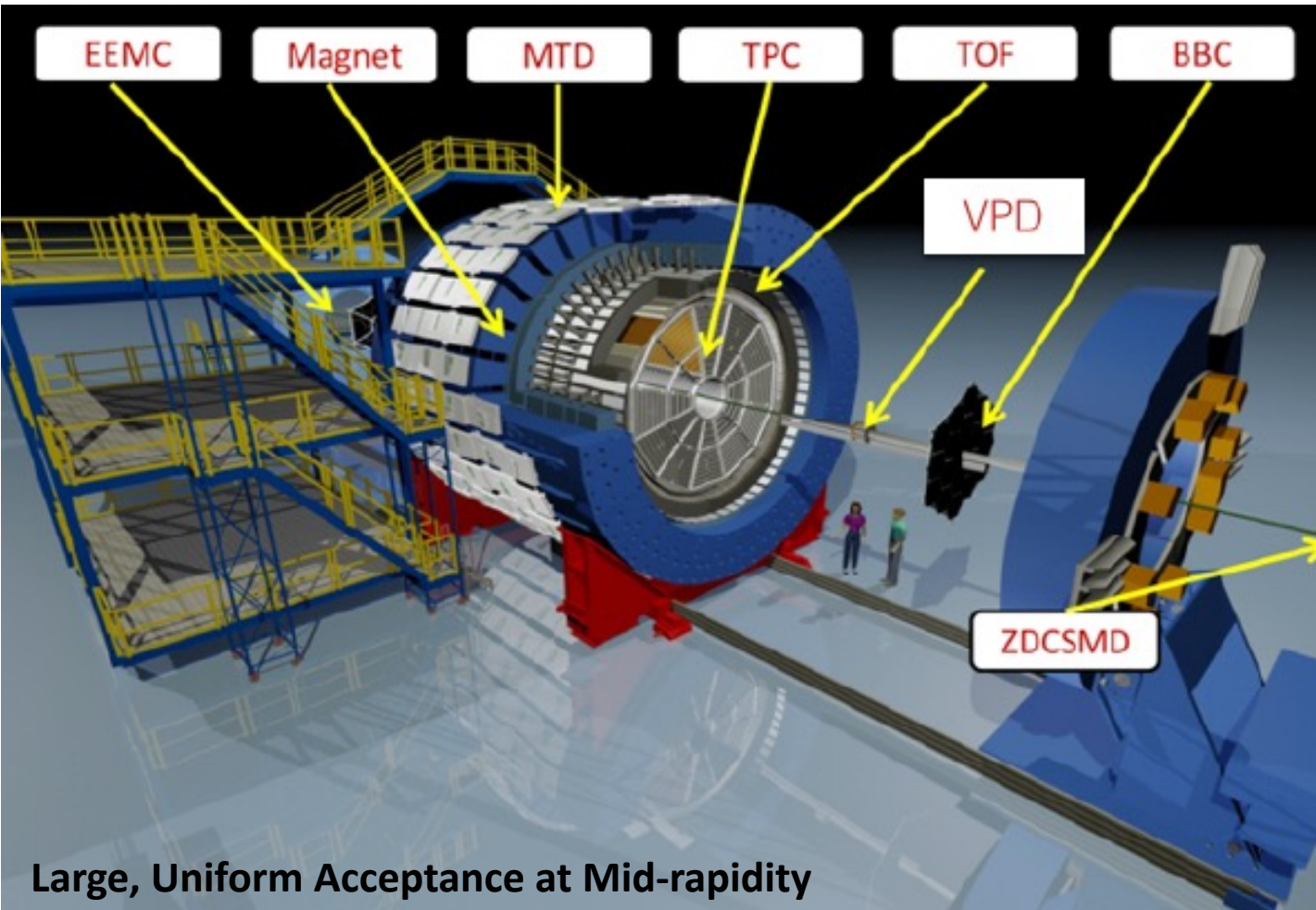
[Möller et al., ADNDT59,185(1995)]

[Hilaire & Girod, EPJA(2007)]

BNL nuclear data center

Heavy-ion collisions could perform a new experimental test of constraint on the uranium β_2 in such a short time-scale ($\sim 10^{-23}\text{s}$).

STAR detector and datasets



Two topics are explored:

(I) Results for the size fluctuation

(II) Results for the v_n - $\langle p_T \rangle$ correlations

- Dataset:

Au+Au@200GeV

U+U@193GeV

- $\langle p_T \rangle$, v_n , N_{ch} are measured within:

$0.2 < p_T < 2.0 \text{ GeV}/c$ and $0.5 < p_T < 2.0 \text{ GeV}/c$

$|\eta| < 1.0$

- Centrality is defined by N_{ch} ($|\eta| < 0.5$).

Observables for the size fluctuation

Mean p_T fluctuations

Mean $[p_T] \equiv \frac{\sum_i w_i p_{T,i}}{\sum_i w_i}, \langle \langle p_T \rangle \rangle \equiv \langle [p_T] \rangle_{\text{evt}} \quad \delta p_T = p_T - \langle \langle p_T \rangle \rangle$

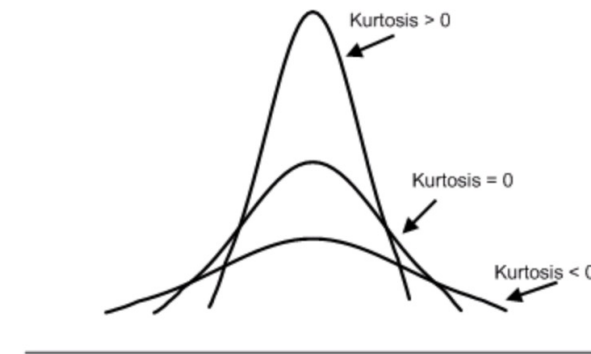
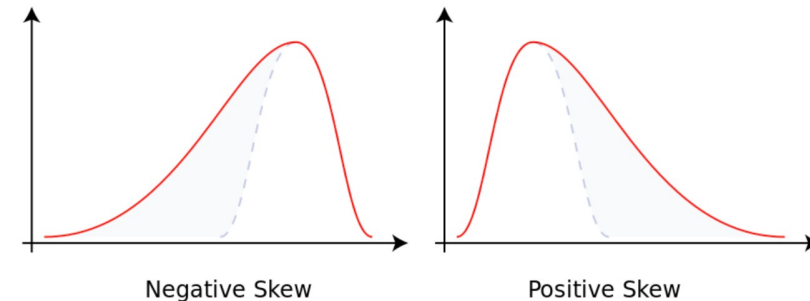
Variance $\langle (\delta p_T)^2 \rangle = \left\langle \frac{\sum_{i \neq j} w_i w_j (p_{T,i} - \langle \langle p_T \rangle \rangle)(p_{T,j} - \langle \langle p_T \rangle \rangle)}{\sum_{i \neq j} w_i w_j} \right\rangle_{\text{evt}}$

skewness $\langle (\delta p_T)^3 \rangle = \left\langle \frac{\sum_{i \neq j \neq k} w_i w_j w_k (p_{T,i} - \langle \langle p_T \rangle \rangle)(p_{T,j} - \langle \langle p_T \rangle \rangle)(p_{T,k} - \langle \langle p_T \rangle \rangle)}{\sum_{i \neq j \neq k} w_i w_j w_k} \right\rangle_{\text{evt}}$

kurtosis $\langle (\delta p_T)^4 \rangle_c = \langle (\delta p_T)^4 \rangle - 3 * \langle (\delta p_T)^2 \rangle^2$

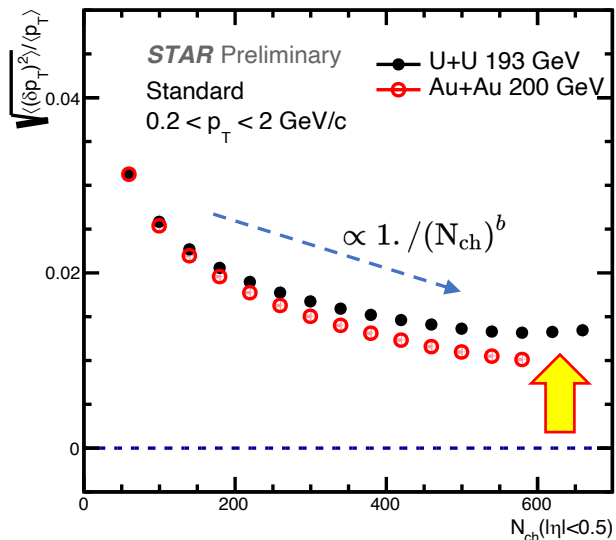
Normalized cumulants:

$$\frac{\sqrt{\langle (\delta p_T)^2 \rangle}}{\langle p_T \rangle}, \quad \frac{\langle (\delta p_T)^3 \rangle}{\langle (\delta p_T)^2 \rangle^{3/2}}, \quad \frac{\langle (\delta p_T)^3 \rangle * \langle p_T \rangle}{\langle (\delta p_T)^2 \rangle^2}, \quad \frac{\langle (\delta p_T)^4 \rangle_c}{\langle (\delta p_T)^2 \rangle^2}$$

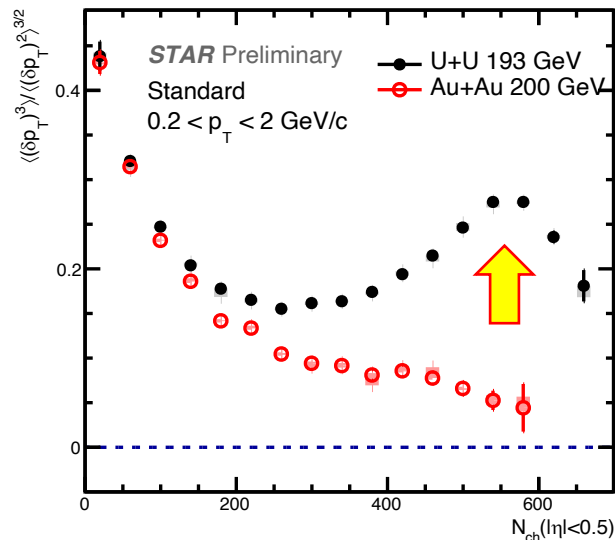


Mean p_T fluctuations

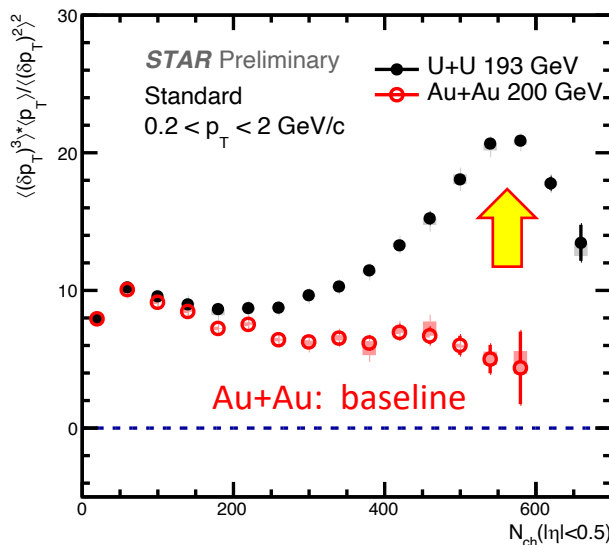
Normalized variance $\sqrt{\frac{\langle (\delta p_T)^2 \rangle}{\langle p_T \rangle}}$



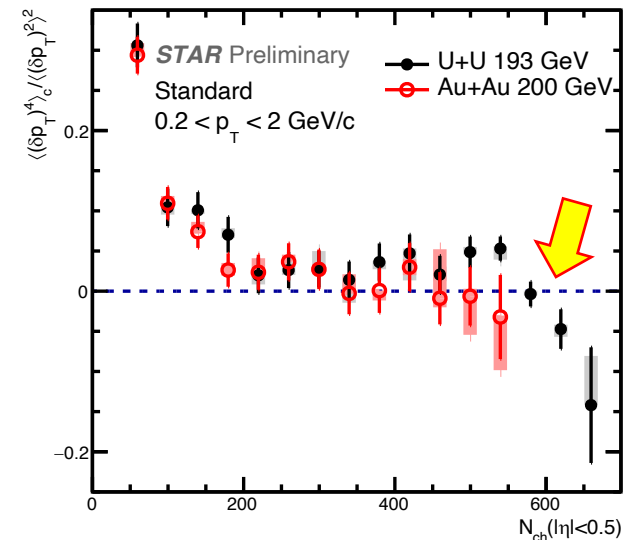
Normalized skewness $\frac{\langle (\delta p_T)^3 \rangle}{\langle (\delta p_T)^2 \rangle^{3/2}}$



Intensive skewness $\frac{\langle (\delta p_T)^3 \rangle * \langle p_T \rangle}{\langle (\delta p_T)^2 \rangle^2}$



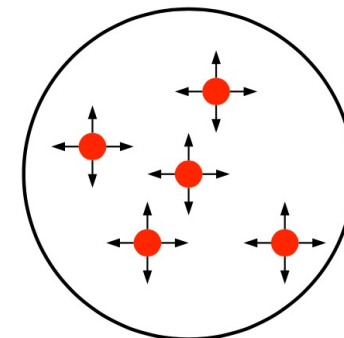
Normalized kurtosis $\frac{\langle (\delta p_T)^4 \rangle_c}{\langle (\delta p_T)^2 \rangle^2}$



Normalized variance and skewness in Au+Au roughly follow a power-law function of N_{ch} .

U+U shows significant enhancement in central region in variance and skewness quantities
 → size fluctuation due to deformation effect.

U+U shows sign-change in normalized kurtosis → size fluctuation due to deformation effect

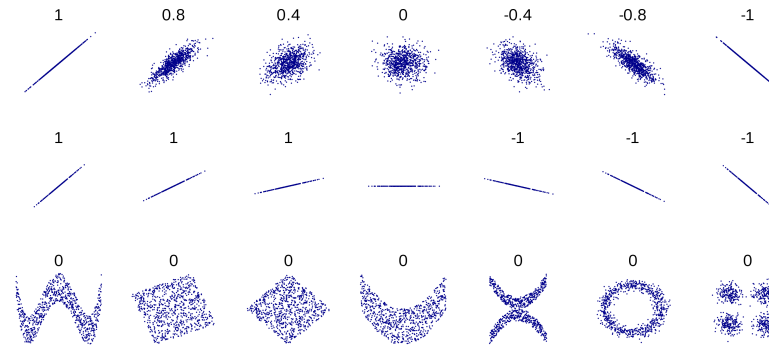


Independent source

Observables for the $v_n - \langle p_T \rangle$ correlations

Pearson correlation coefficient: measuring linear correlation between two variables X and Y .

$$\rho(X, Y) = \frac{\text{cov}(X, Y)}{\sigma_X \sigma_Y}$$



Pearson coefficient: $v_n - p_T$ three particle correlator

$$\rho(v_n^2, [p_T]) = \frac{\text{cov}(v_n^2, [p_T])}{\sqrt{\text{Var}(v_n^2)_{\text{dyn}} \langle \delta p_T \delta p_T \rangle}}$$

$$\text{cov}(v_n^2, [p_T]) \equiv \left\langle \frac{\sum_{i \neq j \neq k} w_i w_j w_k e^{in\phi_i} e^{-in\phi_j} (p_{T,k} - \langle \langle p_T \rangle \rangle)}{\sum_{i \neq j \neq k} w_i w_j w_k} \right\rangle_{\text{evt}}$$

$$[p_T] \equiv \frac{\sum_i w_i p_{T,i}}{\sum_i w_i}, \quad \langle \langle p_T \rangle \rangle \equiv \langle [p_T] \rangle_{\text{evt}}$$

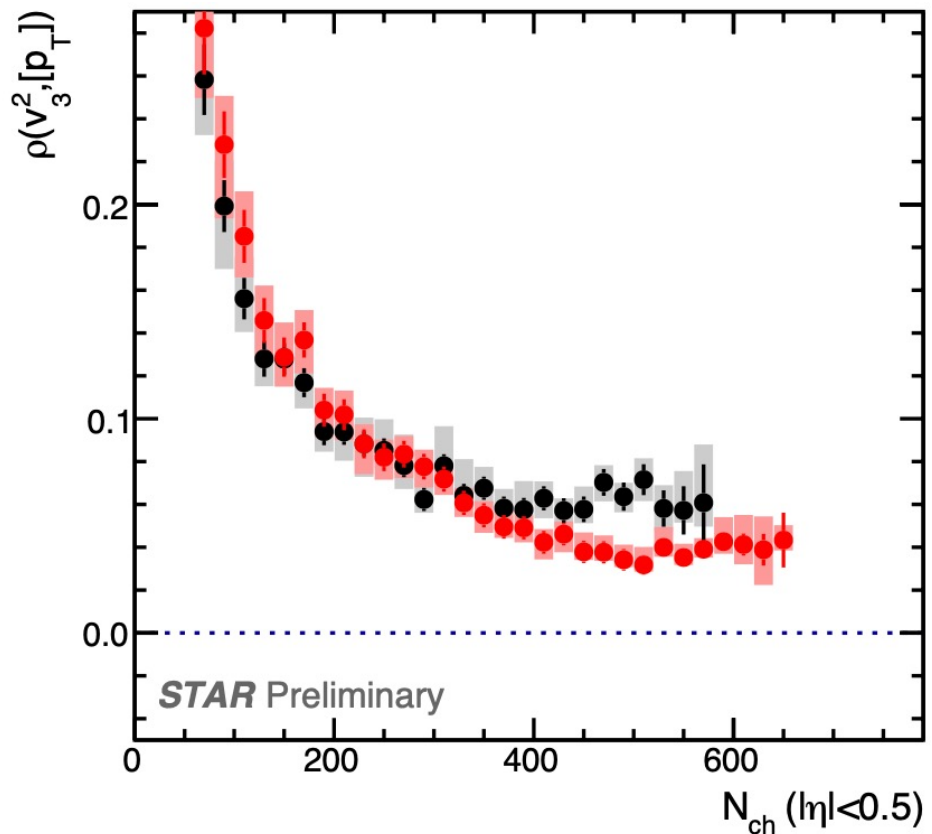
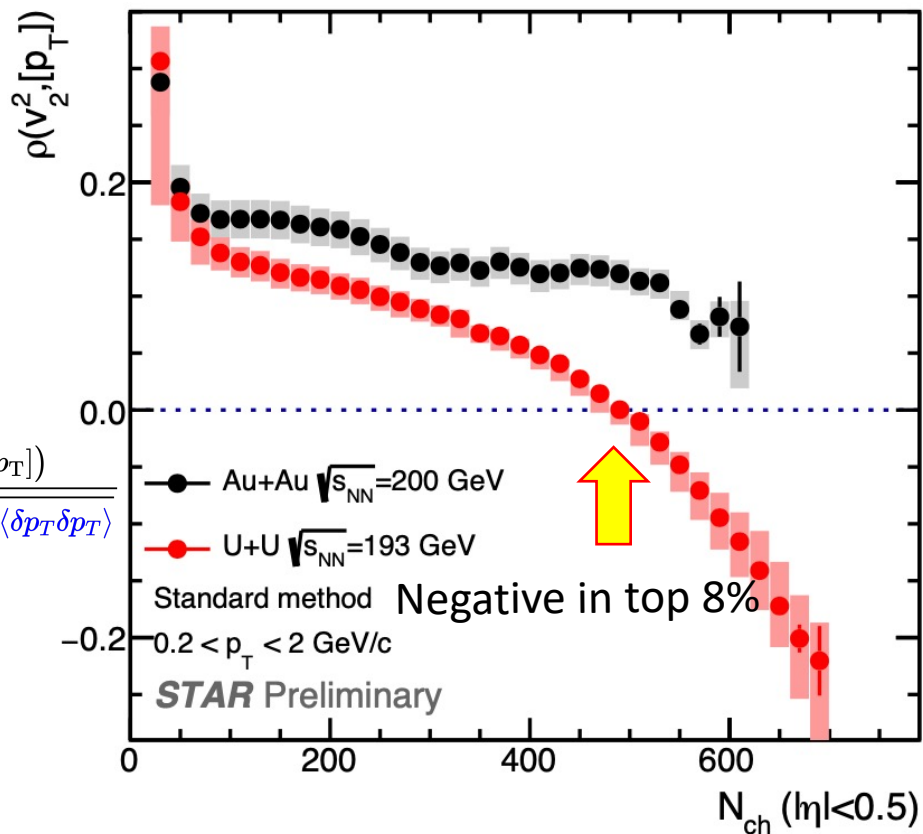
w_i is track weight

$$\text{Var}(v_n^2)_{\text{dyn}} = v_n\{2\}^4 - v_n\{4\}^4$$

$$\langle \delta p_T \delta p_T \rangle = \left\langle \frac{\sum_{i \neq j} w_i w_j (p_{T,i} - \langle \langle p_T \rangle \rangle) (p_{T,j} - \langle \langle p_T \rangle \rangle)}{\sum_{i \neq j} w_i w_j} \right\rangle_{\text{evt}}$$

Pearson coefficient $\rho(v_n^2, [p_T])$

$$\rho(v_n^2, [p_T]) = \frac{\text{cov}(v_n^2, [p_T])}{\sqrt{\text{Var}(v_n^2)_{\text{dyn}} \langle \delta p_T \delta p_T \rangle}}$$

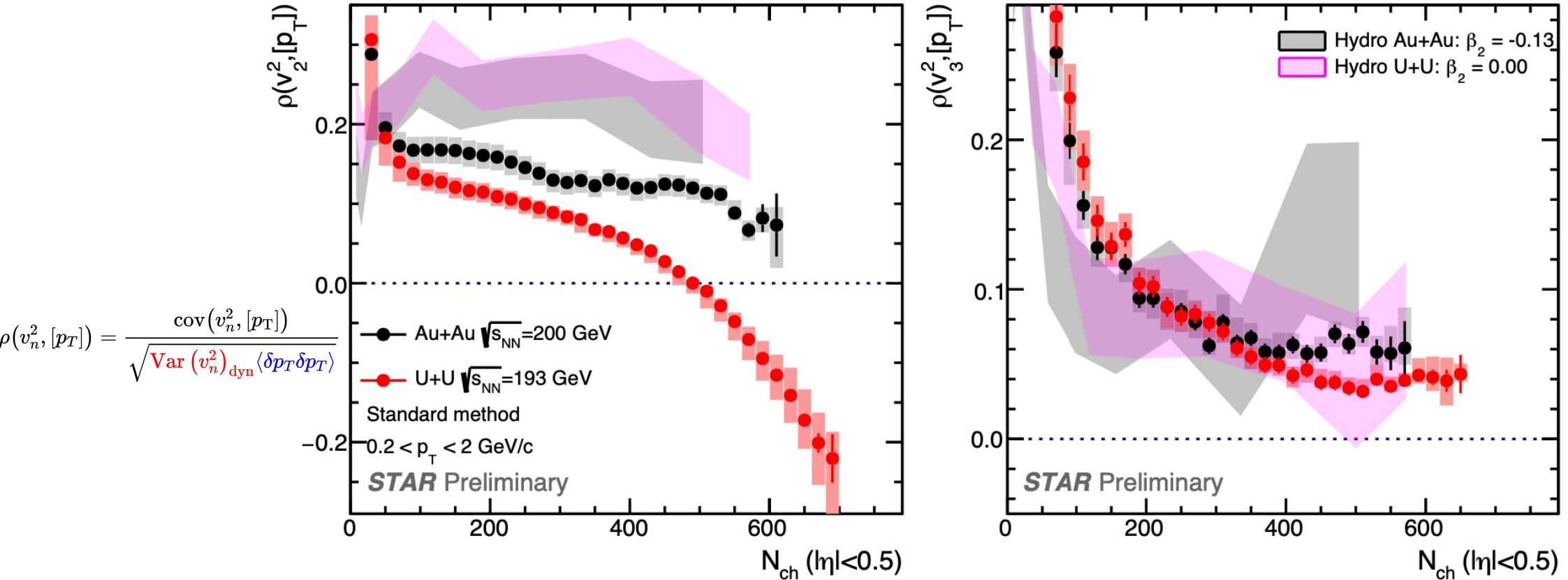


$\rho(v_2^2, [p_T])$ has a clear difference: **negative (anticorrelation)** in U+U central, **positive** in Au+Au central.

$\rho(v_3^2, [p_T])$ is **positive and consistent** in Au+Au and U+U collisions.

$\rho(v_n^2, [p_T])$ compared to IP-Glasma+Hydro

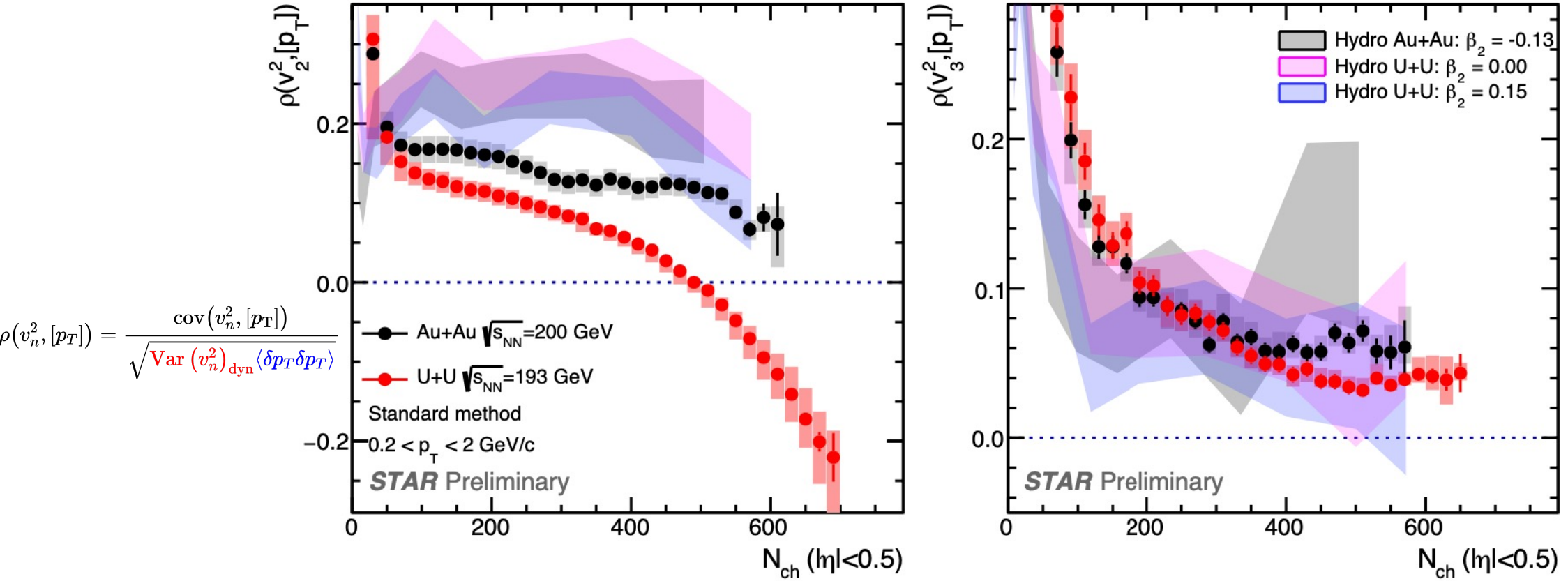
IP-Glasma+Hydro: private calculation provided by Bjoern Schenke (based on B. Schenke, C. Shen, P. Tribedy, [PRC102, 044905\(2020\)](#))



Without deformation, model over-predicts the values for $\rho(v_2^2, [p_T])$.

$\rho(v_n^2, [p_T])$ compared to IP-Glasma+Hydro

IP-Glasma+Hydro: private calculation provided by Bjoern Schenke (based on B. Schenke, C. Shen, P. Tribedy, [PRC102, 044905\(2020\)](#))

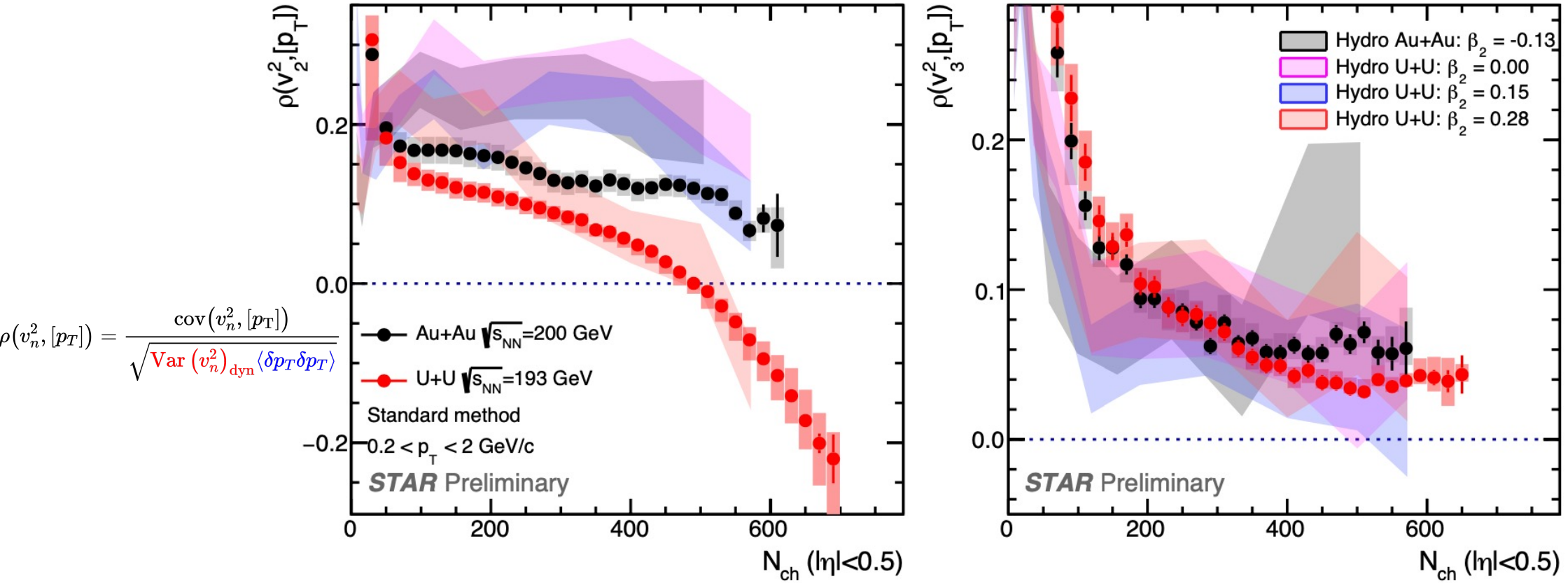


Without deformation, model over-predicts the values for $\rho(v_2^2, [p_T])$.

With increasing β_2 , model roughly describes the trend of $\rho(v_2^2, [p_T])$.

$\rho(v_n^2, [p_T])$ compared to IP-Glasma+Hydro

IP-Glasma+Hydro: private calculation provided by Bjoern Schenke (based on B. Schenke, C. Shen, P. Tribedy, [PRC102, 044905\(2020\)](#))

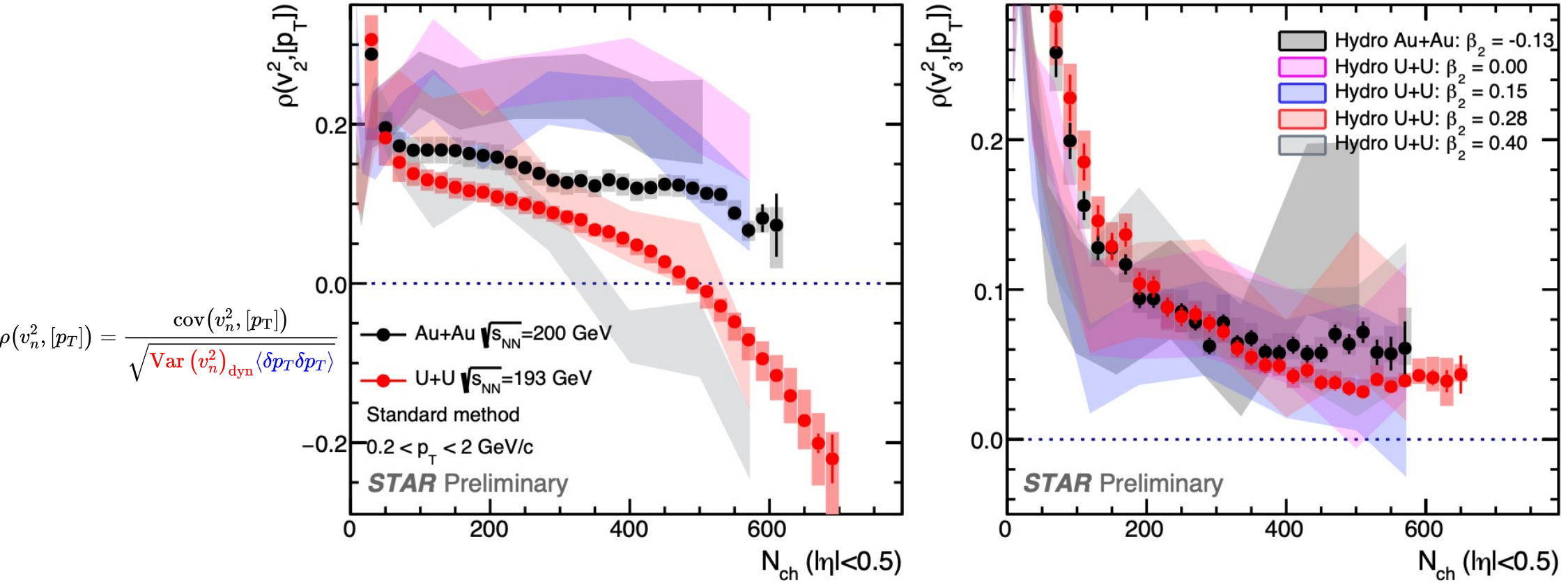


Without deformation, model over-predicts the values for $\rho(v_2^2, [p_T])$.

With increasing β_2 , model roughly describes the trend of $\rho(v_2^2, [p_T])$.

$\rho(v_n^2, [p_T])$ compared to IP-Glasma+Hydro

IP-Glasma+Hydro: private calculation provided by Bjoern Schenke (based on B. Schenke, C. Shen, P. Tribedy, [PRC102, 044905\(2020\)](#))



Without deformation, model over-predicts the values for $\rho(v_2^2, [p_T])$.

With increasing β_2 , model roughly describes the trend of $\rho(v_2^2, [p_T])$.

Model shows that $\rho(v_3^2, [p_T])$ are insensitive to β_2 .

The sign-change is due to deformation effect and model quantifies the β_2 value around $0.28 < \beta_2 < 0.4$

Conclusions and outlooks

1. $[p_T]$ fluctuations:

- Show sensitivity to quadruple deformation β_2 .
- Strong increase of variance, skewness and negative kurtosis towards central U+U.

$$\rho(r, \theta) = \frac{\rho_0}{1 + e^{(r-R_0(1+\beta_2 Y_{20}(\theta)))/a}}$$

2. v_n - $[p_T]$ correlations:

- Strong suppression and sign-change for $n=2$ in U+U, but no difference for $n=3$ in Au+Au and U+U.
- Deformation influences collisions over a wide centrality range: mid-central to central.
- Subevent method could decrease non-flow contributions in peripheral collisions.
- Main features are robust against p_T selection.

3. Qualitatively described by IP-Glasma+MUSIC+UrQMD calculations:

- Prefer a quadrupole deformation of $0.28 \leq \beta_2 \leq 0.40$.
- Help model to constrain the initial conditions.
- Open up an avenue for studying nuclear shape in heavy-ion collisions.

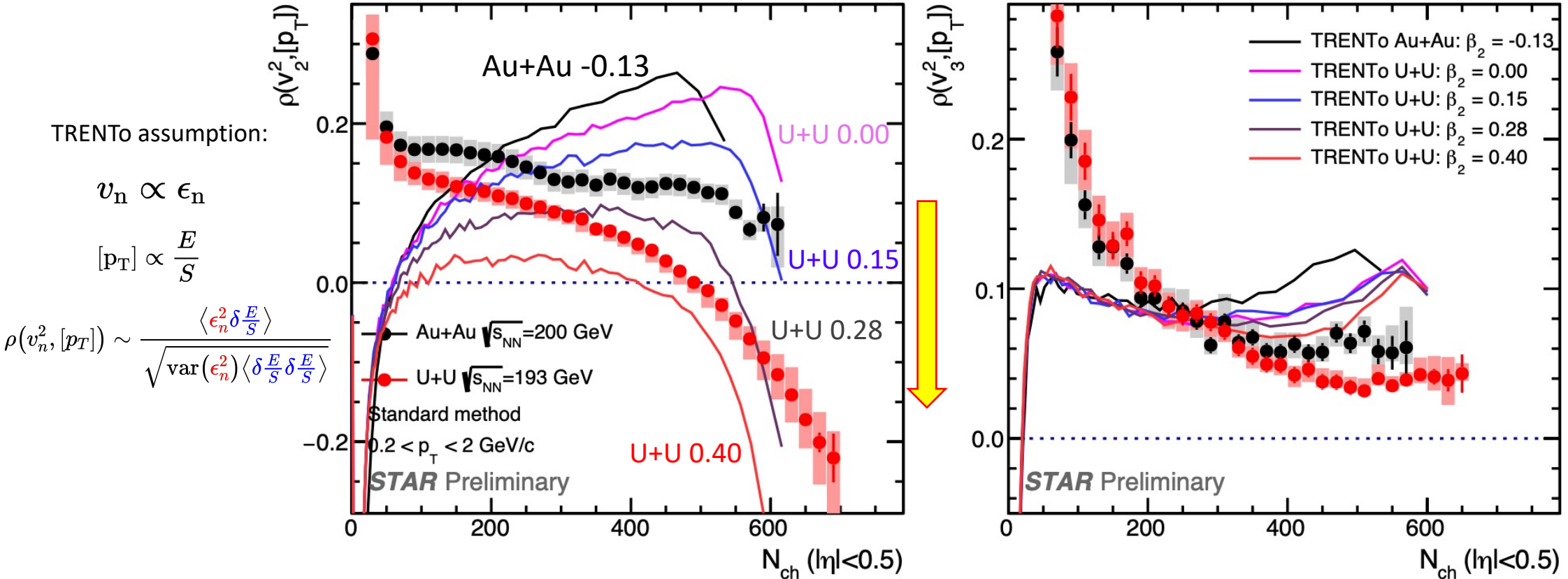
4. Outlooks: isobar collisions and small system collisions could address two questions

- Could decipher the puzzle of nuclear deformation in Ru and Zr.
- Could study the initial state momentum anisotropy from the CGC prediction.

Many thanks to APS and also thank you for listening.

$\rho(v_n^2, [p_T])$ compared to TRENTo initial condition model

TRENTo: private calculation provided by Giuliano Giacalone (based on [PRC102, 024901\(2020\)](#), [PRL124, 202301\(2020\)](#))



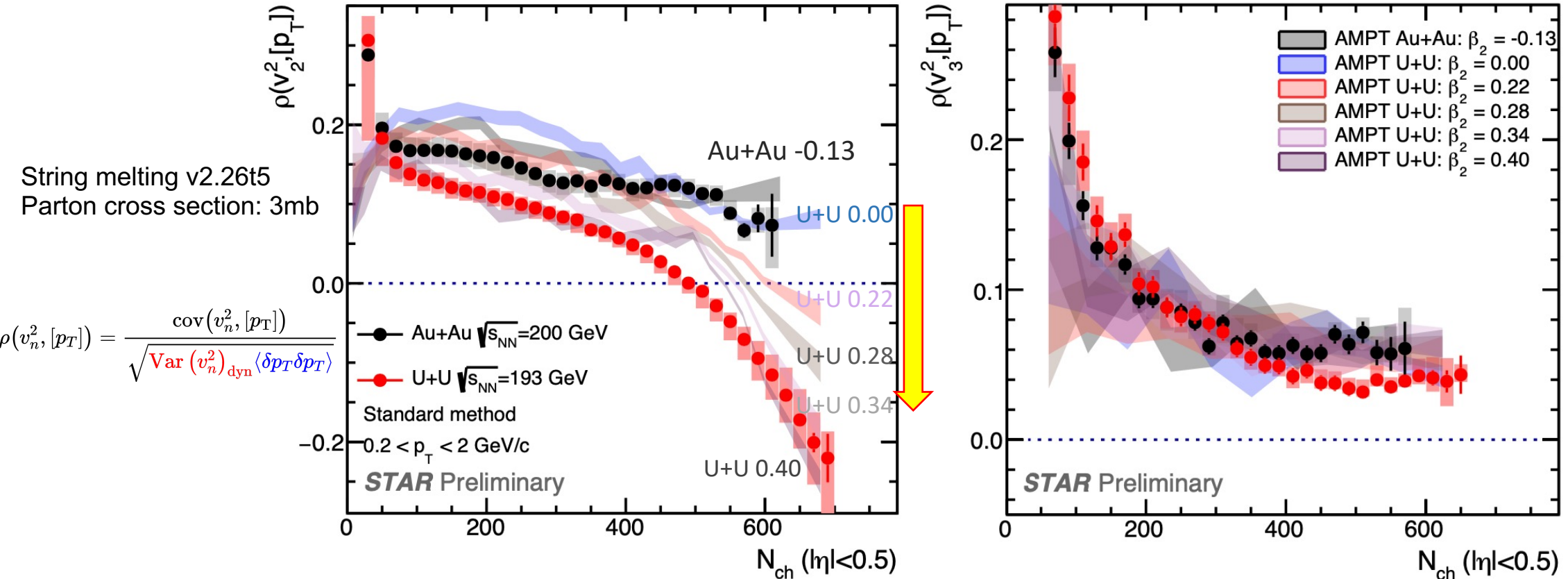
TRENTo fails to describe the STAR data but shows a **hierarchical β_2 dependence** in U+U collisions.

TRENTo suggests this sign-change in central U+U collisions **due to deformation effect, and prefers $0.28 < \beta_2 < 0.4$**

TRENTo shows that $\rho(v_3^2, [p_T])$ is **insensitive** to the nuclear deformation effects.

$\rho(v_n^2, [p_T])$ compared to transport AMPT model

AMPT: Chunjian Zhang, Jianguong Jia et al., (In preparation)



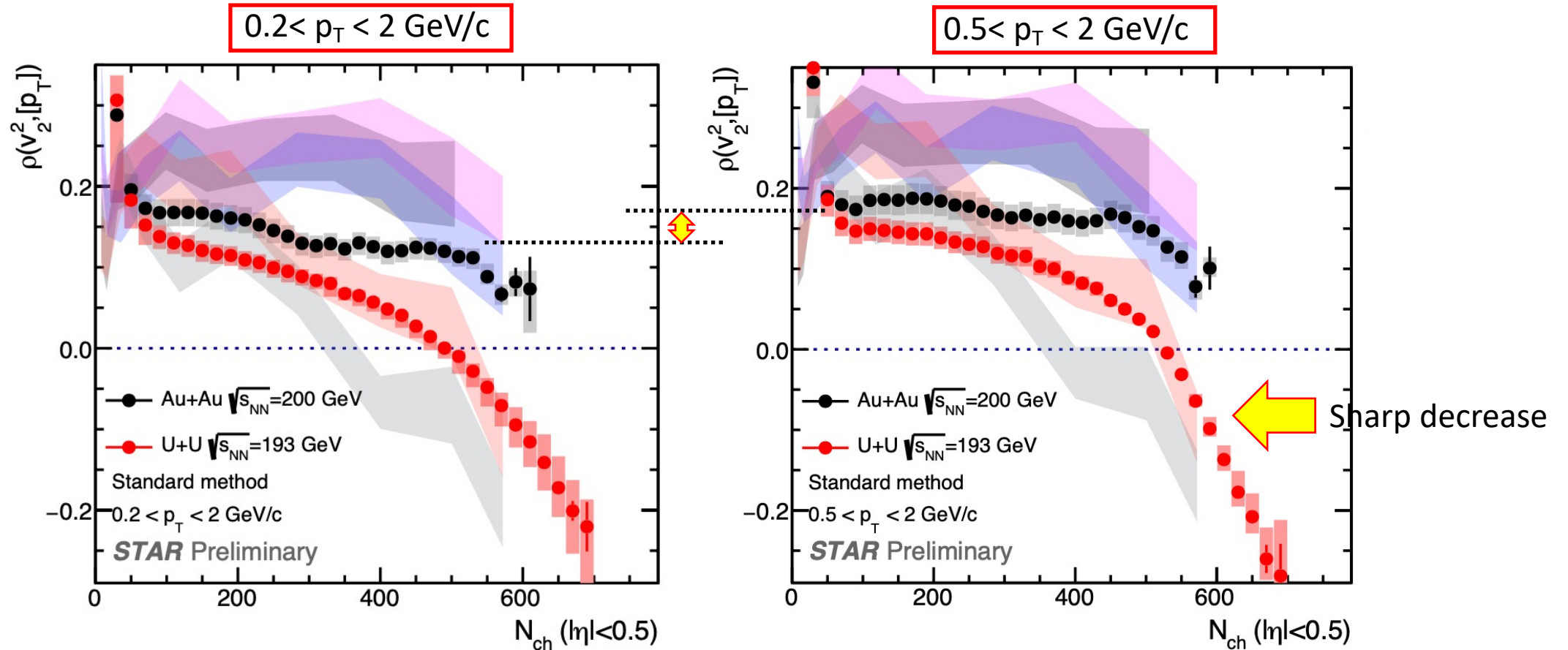
AMPT shows a clear β_2 dependence in Uranium $\rho(v_2^2, [p_T])$ while not in $\rho(v_3^2, [p_T])$.

AMPT also supports the sign-change of $\rho(v_2^2, [p_T])$ in U+U is due to deformation effect.

AMPT favors the β_2 value around $0.28 < \beta_2 < 0.4$ for uranium.

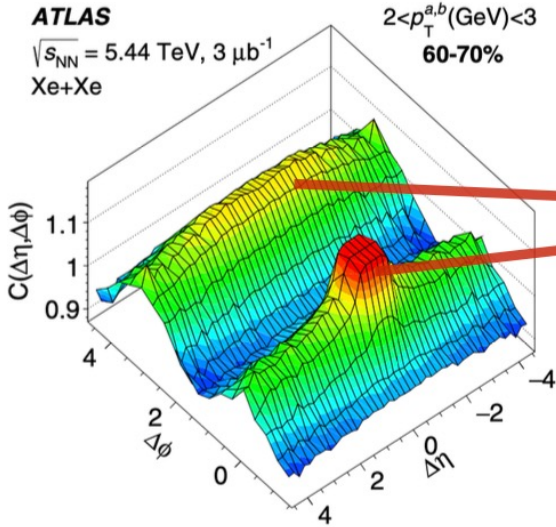
$\rho(v_n^2, [p_T])$ in different p_T selection

IP-Glasma+Hydro: private calculation provided by Bjoern Schenke (based on B. Schenke, C. Shen, P. Tribedy, [PRC102, 044905\(2020\)](#))

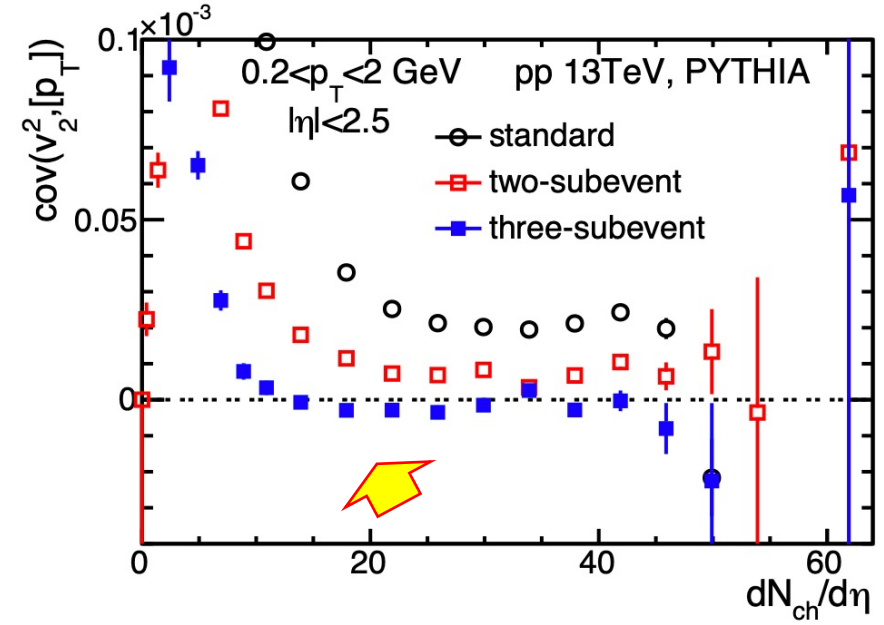


Features are same for $0.5 < p_T < 2$ GeV/c as $0.2 < p_T < 2$ GeV/c.

Non-flow suppression



Short range correlations:
 jets, resonance decays, HBT, etc.



C.J. Zhang et al, [arXiv:2102.05200](https://arxiv.org/abs/2102.05200)

non-flow suppression via subevent methods by correlating particles from different η windows

Full event

$$v_2, p_T \mid |\eta| < 1.0$$

Two-subevent

$$v_2^A \mid \eta < -0.1$$

$$v_2^B \mid \eta > 0.1$$

Three-subevent

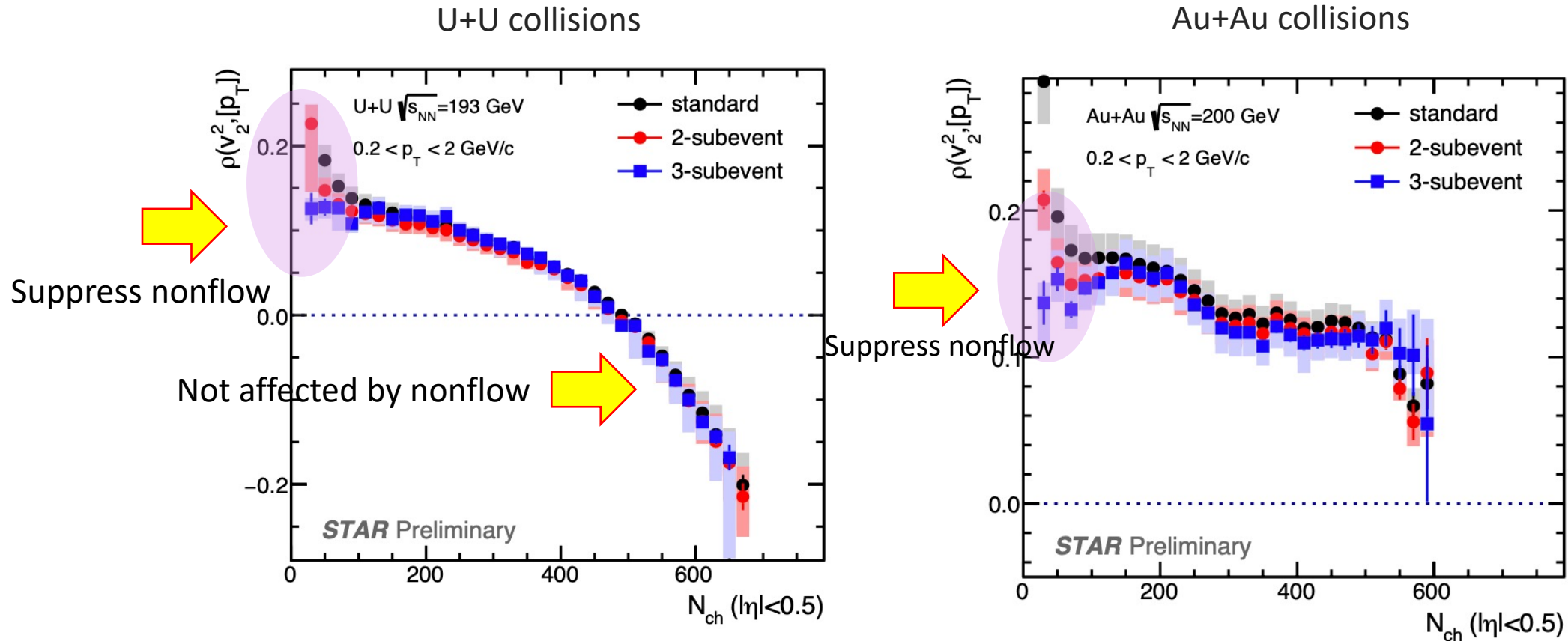
$$v_2^A \mid \eta < -0.35$$

$$v_2^B \mid |\eta| < 0.3$$

$$v_2^C \mid \eta > 0.35$$

Non-flow effect is important in peripheral region and they are greatly suppressed using subevent method.

The effects of non-flow in $\rho(v_n^2, [p_T])$



Standard method is consistent with subevent methods at high N_{ch} .

Subevent methods could decrease non-flow contributions in peripheral collisions.

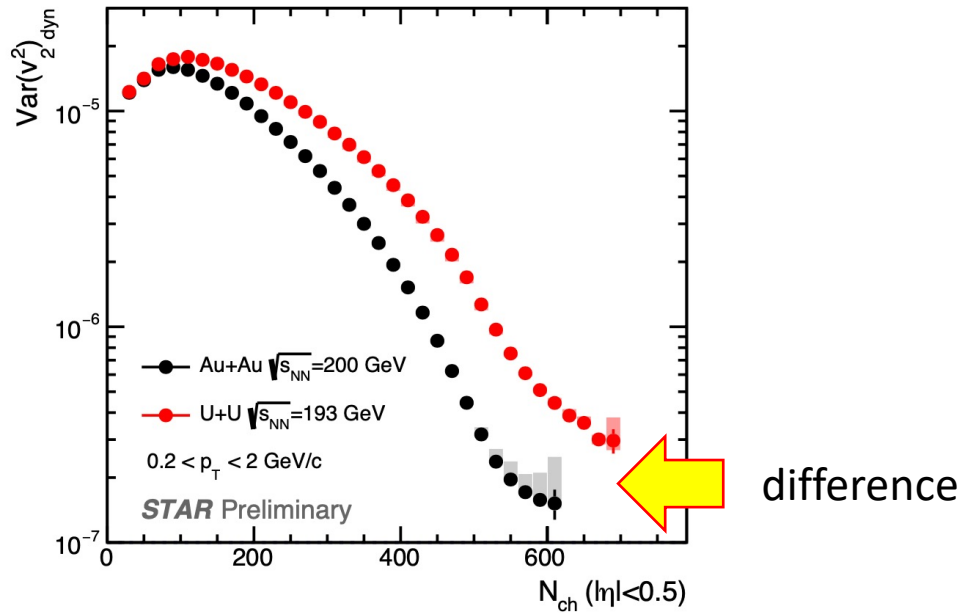
Non-flow effect is not responsible for the sign-change in U+U collisions.

Dynamical v_n^2 variance and $\langle p_T \rangle$ fluctuations

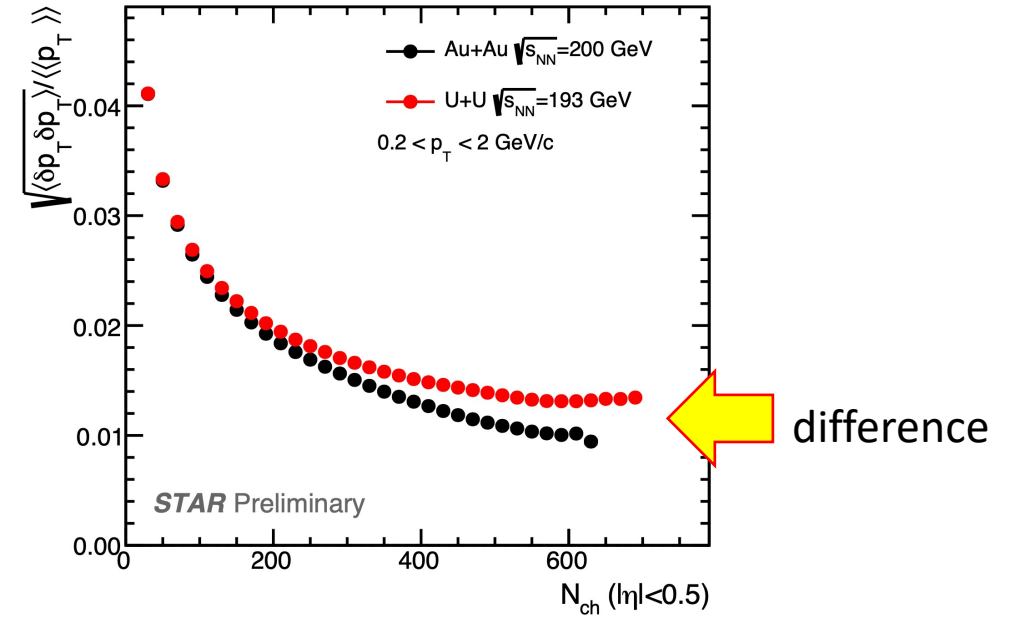
$$\rho(v_n^2, [p_T]) = \frac{\text{cov}(v_n^2, [p_T])}{\sqrt{\text{Var}(v_n^2)_{\text{dyn}} \langle \delta p_T \delta p_T \rangle}}$$

$$\text{Var}(v_n^2)_{\text{dyn}} = v_n\{2\}^4 - v_n\{4\}^4$$

$$\langle \delta p_T \delta p_T \rangle = \left\langle \frac{\sum_{i \neq j} w_i w_j (p_{T,i} - \langle p_T \rangle)(p_{T,j} - \langle p_T \rangle)}{\sum_{i \neq j} w_i w_j} \right\rangle_{\text{evt}}$$



difference of flow fluctuation due to deformation.

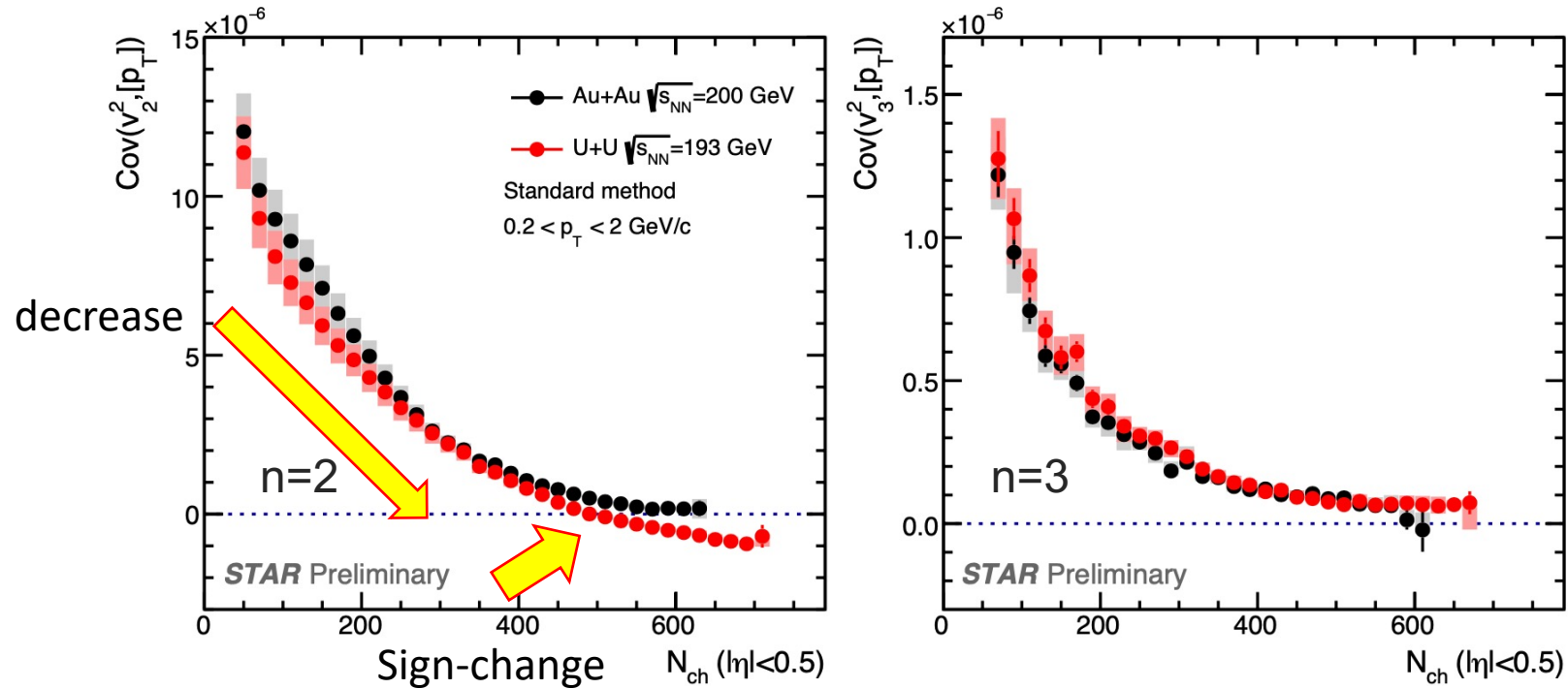


difference of $\langle p_T \rangle$ fluctuation due to deformation.

Nuclear deformation plays a role in flow and $\langle p_T \rangle$ fluctuations.

Covariance $\text{Cov}(v_n^2, [p_T])$

$$\rho(v_n^2, [p_T]) = \frac{\text{cov}(v_n^2, [p_T])}{\sqrt{\text{Var}(v_n^2)_{\text{dyn}} \langle \delta p_T \delta p_T \rangle}} \rightarrow \text{cov}(v_n^2, [p_T]) \equiv \left\langle \frac{\sum_{i \neq j \neq k} w_i w_j w_k e^{in\phi_i} e^{-in\phi_j} (p_{T,k} - \langle p_T \rangle)}{\sum_{i \neq j \neq k} w_i w_j w_k} \right\rangle_{\text{evt}}$$

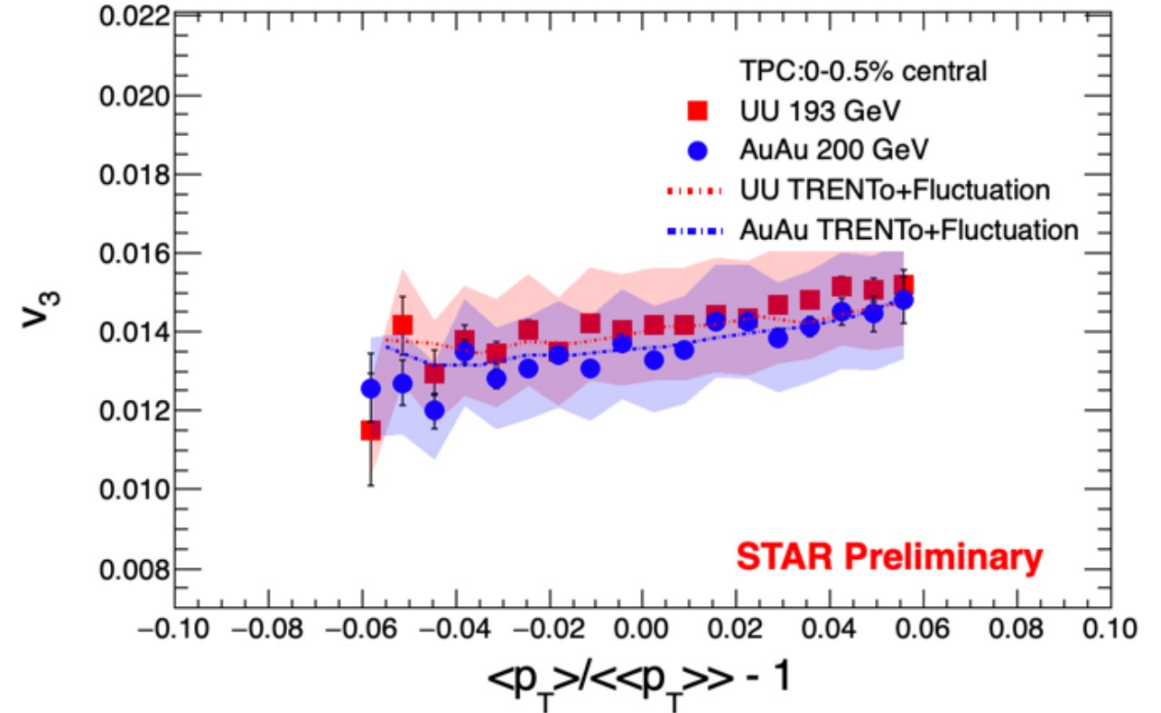
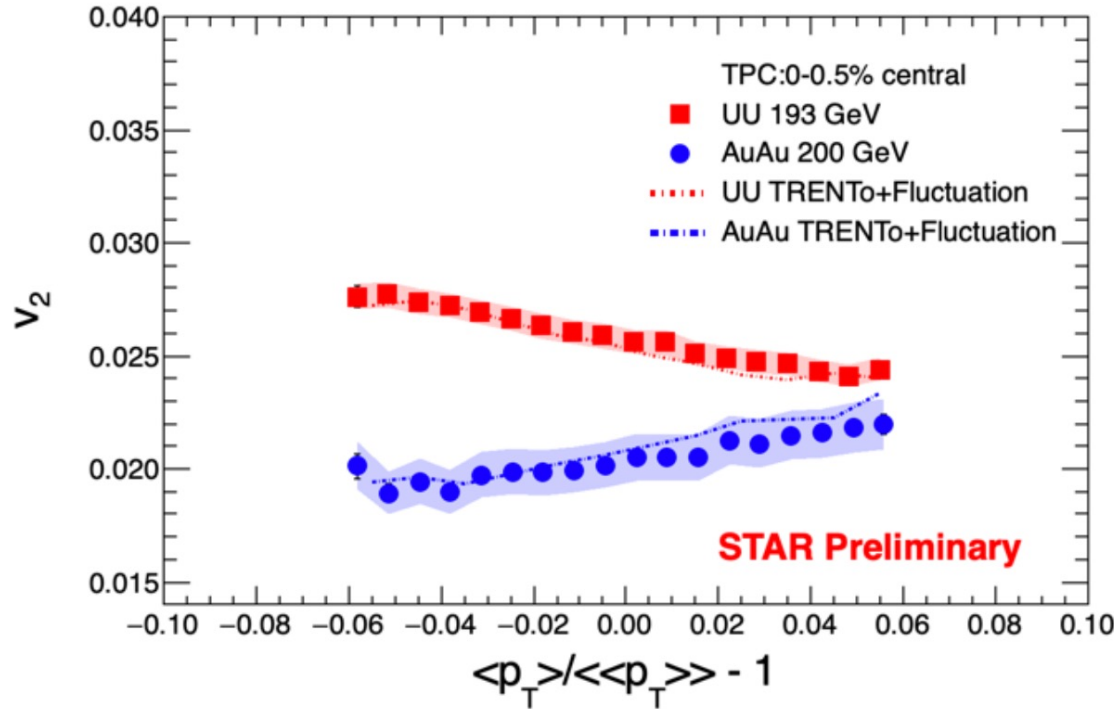


U+U collisions show a sign-change behavior in $\text{Cov}(v_2^2, [p_T])$ while not in Au+Au. But they are consistent for $\text{Cov}(v_3^2, [p_T])$.

This sign-change behavior indicates the effect of deformation.

Event-by-event v_n vs. $\langle p_T \rangle$ in ultra central (0-0.5%) collisions

WWND2020, Shengli Huang (STAR Collaboration)



v_n	System	slope
v_2	U + U	$-3.5\% \pm 0.1\%$
v_2	Au + Au	$2.6\% \pm 0.2\%$
v_3	U + U	$1.7\% \pm 0.2\%$
v_3	Au + Au	$1.9\% \pm 0.2\%$

An **anticorrelation** is observed between v_2 and $\langle p_T \rangle$ in top 0.5% U+U collisions while not in Au+Au.

v_3 and $\langle p_T \rangle$ correlations are **positive and similar** for Au+Au and U+U collisions.

After incorporating the statistical fluctuation due to finite multiplicity, the TRENTo model can reproduce the data quantitatively.

The anticorrelation in v_2 vs. $\langle p_T \rangle$ for U+U is due to deformation.